

Kcnh2 deletion is associated with rat embryonic development defects via destruction of KCNH2-integrin β 1 complex

SANGYU HU^{1-3*}, ZHIGANG LI^{1-3*}, HUAN LIU¹⁻³, WENZE CAO¹⁻³, YILEI MENG¹⁻³, CHANG LIU¹⁻³, SIYU HE¹⁻³, QIN LIN¹⁻³, MENGYUE SHANG¹⁻³, FANG LIN¹⁻³, NA YI¹⁻³, HANRUI WANG¹⁻³, AGAPIOS SACHINIDIS⁴, QILONG YING⁵, LI LI^{1-3,6,7} and LUYING PENG^{1-3,6,7}

¹State Key Laboratory of Cardiology, Shanghai East Hospital, Tongji University School of Medicine, Shanghai 200120;

²Institute of Medical Genetics, Tongji University, Shanghai 200331; ³Heart Health Center, Shanghai East Hospital,

Tongji University School of Medicine, Shanghai 200120, P.R. China; ⁴University of Cologne, Faculty of Medicine and University Hospital Cologne, Center for Physiology, Working Group Sachinidis, Center for Molecular Medicine, D-50931 Cologne, Germany; ⁵Eli and Edythe Broad Center for Regenerative Medicine and Stem Cell Research, Department of Stem Cell Biology and Regenerative Medicine, Keck School of Medicine, University of Southern California, Los Angeles, CA 90033, USA; ⁶Research Units of Origin and Regulation of Heart Rhythm, Chinese Academy of Medical Sciences, Beijing 100730; ⁷Department of Medical Genetics Tongji University School of Medicine, Shanghai 200331, P.R. China

Received May 18, 2023; Accepted October 6, 2023

DOI: 10.3892/ijmm.2023.5338

Abstract. The Kv11.1 potassium channel encoded by the *Kcnh2* gene is crucial in conducting the rapid delayed rectifier K⁺ current in cardiomyocytes. Homozygous mutation in *Kcnh2* is embryonically lethal in humans and mice. However, the molecular signaling pathway of intrauterine fetal loss is unclear. The present study generated a *Kcnh2* knockout rat based on edited rat embryonic stem cells (rESCs). *Kcnh2* knockout was embryonic lethal on day 11.5 of development due to a heart configuration defect. Experiments with human embryonic heart single cells (6.5-7 weeks post-conception) suggested that potassium voltage-gated channel subfamily H member 2 (KCNH2) plays a crucial role in the development of compact cardiomyocytes. By contrast, apoptosis was found to be triggered in the homozygous embryos, which could be attributed to the failure of KCNH2 to form a complex with integrin β 1 that was essential for preventing the process of apoptosis via inhibition of forkhead box O3A. Destruction of the KCNH2/integrin β 1 complex reduced the phosphorylation level of AKT and deactivated the glycogen synthase kinase 3 β (GSK-3 β)/ β -catenin pathway, which caused early

developmental abnormalities in rats. The present work reveals a basic mechanism by which KCNH2 maintains intact embryonic heart development.

Introduction

The human ether-a-go-go-related gene (*Kcnh2*) encodes for the Kv11.1 potassium channel which conducts the rapidly activating delayed rectifier K⁺ current (IKr) in the heart (1,2). It has been reported that potassium voltage-gated channel subfamily H member 2 (KCNH2) plays a fundamental role in the rapid delayed rectifier K⁺ current, which is associated with cardiac arrhythmia (3). KCNH2 has also been shown to be involved in regulating cell proliferation, apoptosis, cell invasion and angiogenesis (4).

Nonsense *Kcnh2* mutation was recently found to be responsible for inducing intrauterine fetal loss in humans (5,6), which indicates the critical role of KCNH2 in embryo development. However, the underlying mechanisms are still unknown. KCNH2 has been shown to regulate apoptosis and cell proliferation by interacting with integrin β 1 and this engagement can enhance membrane insertion and activation of KCNH2 in acute myeloid leukemia (7). Integrin β 1 is associated with the development of the vascular and nervous systems (8). KCNH2, integrin β 1 and focal adhesion kinase (FAK) form a macromolecular complex and activation of KCNH2 channels is essential for mediating FAK activity, which then regulates cell survival and prevents apoptosis. However, the association between KCNH2 and integrin β 1 is cell type- and context-dependent. For instance, dissociation of KCNH2 and integrin β 1 has been found to occur in adult cardiomyocytes due to interruption of KCNE1 (9). Reducing the current activity of KCNH2 *in vitro* can promote apoptosis and result in cell cycle arrest (10,11). Even inhibition of KCNH2 has been shown to activate a variety of apoptotic pathways, such as endoplasmic reticulum,

Correspondence to: Professor Li Li or Professor Luying Peng, State Key Laboratory of Cardiology, Shanghai East Hospital, Tongji University School of Medicine, 500 Zhennan Road, Putuo, Shanghai 200120, P.R. China
E-mail: lilirz@tongji.edu.cn
E-mail: luyingpeng@tongji.edu.cn

*Contributed equally

Key words: embryonic development, *Kcnh2*, integrin β 1, AKT

MAPK and FAK pathways (12). Our previous findings have demonstrated that KCNH2 interacts with integrin β 1 to regulate the differentiation of rat embryonic stem cells (rESCs) into cardiomyocytes (13). However, the interaction mechanisms that maintain embryo and cardiac development *in vitro* still need to be further explored.

The AKT pathway has been shown to regulate cardiovascular development processes such as growth, differentiation and apoptosis (14). Our recent study also found that loss of function of KCNH2 aggravated cardiac dysfunction induced by lipopolysaccharide via FAK/AKT-forkhead box O3A (FOXO3A) in adult rats (15). KCNH2 can maintain the AKT/IKK β /NF- κ B pathway to inhibit apoptosis during rESC differentiation *in vitro* (13). However, the *in vivo* regulatory mechanism of KCNH2 in embryonic cardiac development is poorly understood.

The present study generated *Kcnh2* knockout (*Kcnh2*^{-/-}) rats via homologous recombination in rESCs. The *Kcnh2*^{-/-} rats reached only the E15 embryonic state with clear cardiac defects, which were associated with inhibition of compact cardiomyocyte development. In addition, *Kcnh2* depletion caused the loss of association with integrin β 1 to form macromolecular complexes that failed to phosphorylate FAK to activate AKT, thereby resulting in stagnation of normal cardiac development.

Materials and methods

Animals. A total of 58 rats were used for animal experiments (all 8 weeks old; weight 200-230 g). A total of four female Fischer 344 rats, five male Fischer 344 rats, four female Sprague-Dawley rats and five male vasectomized Sprague-Dawley rats were purchased from Envigo for performing *Kcnh2* knockout. A total of 20 wild type (WT) and 20 *Kcnh2*^{+/-} female rats were used for isolating embryos at different time points. The animal experiments were performed according to the investigator's protocols approved by the University of Southern California and Tongji University Institutional Animal Care and Use Committee (approval no. TJLAC-016-022) and complied with the AVMA euthanasia guidelines 2020 (<https://olaw.nih.gov/policies-laws/avma-guidelines-2020.htm>). All rats were raised under normal temperature (25°C), normal oxygen conditions (~21%) and normal relative humidity (50%) with a 12-h light/dark cycle. CO₂ with a flow rate of 9 l (30% of the chamber) per min was used to euthanize pregnant rats for isolation of blastocysts or embryos. The detail of the electrocardiograph, echocardiography and whole-cell patch-clamp can be found in the Data S1.

Generation of *Kcnh2* knockout rats. DAc8 rat ES cell line was used and cultured as previously described (16,17). Briefly, the rat ES cells were cultured in 2i medium (18,19) and transfected by electroporation of targeting vector. Puromycin (0.5 μ g/ml; Beyotime Institute of Biotechnology) was used to screen of drug-resistant rat embryonic stem cell colonies. The genome of puromycin-resistant cell colonies was extracted with genomic DNA kit (Tiangen Biotech Co., Ltd.) and PCR was performed using LA Taq (Takara Biotechnology Co., Ltd.). The following thermocycling conditions were applied for 35 cycles: 98°C, 20 sec; T_m, 20 sec; 72°C, 1 kb/min. The products were separated in 1% agarose gel. Colonies that were positive in PCR

were confirmed by Southern blotting. The genomic DNA of rat ES cells was digested by enzyme, separated by agarose gel electrophoresis and transferred to a piece of nylon (Beyotime Institute of Biotechnology). Then, 1.5 μ g of probe was added to 30 ml of buffer for hybridization. F344 blastocysts were isolated from pregnant female Fischer 344 rats. Targeted-ES cell colonies were expanded and injected into F344 blastocysts. The obtained chimeric blastocysts were then transplanted into the uterus of pseudopregnant rats. Generally, 8-10 chimeric blastocysts were transplanted into each pseudopregnant rat. Male chimaeras were mated with SD female rats to generate germline offspring. *Kcnh2* heterozygotes were mated with each other to produce homozygotes. Genomic DNA from rat tail tips were extracted and separated as described previously for genotyping. The sequences of primers are listed in Table I.

RNA isolation and reverse transcription-quantitative (RT-q) PCR. For PCR, 1 ml of Total RNA Extraction Reagent (Shanghai Yeasen Biotechnology Co., Ltd.) was used to extract the total RNA from 100 mg of tissue. The 1st Strand cDNA Synthesis kit, gDNA Digester Plus (Shanghai Yeasen Biotechnology Co., Ltd.) was applied for reverse transcription of total RNA. The reaction program involved heating to 95°C for denaturation and holding at 4°C for 40 cycles (95°C, 15 sec; 55-60°C, 10 sec; 72°C, 20 sec). RT-qPCR was performed using SYBR Green Master Mix (Shanghai Yeasen Biotechnology Co., Ltd.). All procedures were performed according to the manufacturer's protocols. GAPDH was applied to normalize the expression of mRNAs. The experiment was repeated 3 times for each sample. The Ct (threshold cycle) was defined as the number of cycles required for the fluorescence signal to exceed the detection threshold. The 2^{- $\Delta\Delta$ C_t} method was used to calculate the differential expression of genes (20). The related primers are listed in Table S1.

Histological analysis and immunofluorescence. Embryos from *Kcnh2*^{-/-} and WT rats were fixed in 4% paraformaldehyde for 1 h at room temperature. Tissue was dehydrated using ethanol at different concentrations (50, 75, 80, 95 and 100%) for 20 min each for histological analysis. Ethanol was exchanged with xylene twice and the xylene exchanged with paraffin twice, for 1-2 h per exchange. Finally, embryos were embedded in fresh paraffin. Tissue was rehydrated using 10% sucrose and 30% sucrose for 4 h each at 4°C for immunofluorescence. Equal volumes of OCT and 30% sucrose were incubated at room temperature for 30 min, and the tissues were transferred into mold. After paraffin/OCT-embedding, tissue sections were cut at 8-10 μ m. The paraffin sections were stained with hematoxylin and eosin (MilliporeSigma). After permeabilization with 0.1% Triton X-100 and blocking, the OCT sections were stained with the indicated antibodies for 18 h at 4°C (see Table SII for antibody list).

Western blotting. Proteins were extracted from 100 mg of tissue using 1 ml of ice-cold RIPA buffer containing fresh protease and phosphatase inhibitors (Beyotime Institute of Biotechnology) and the concentrations were measured using a BCA assay (Beyotime Institute of Biotechnology). Gels were prepared with a PAGE Gel Fast Preparation kit (Epizyme) according to the manufacturer's instructions. Then, 10 μ g of

Table I. Primer sequences used in screening and genotyping and probe sequence used in southern blotting.

Name	Sequence (5'-3')
sc-F	CATACGAGCCGGAAGCATAAAGTG
sc-R	AGCAGGGTTCGAGTGTCTGTAAAG
probe-F	CCAGACGATATGGTCCTGGATTTG
probe-R	AACAGAATGAGCCAGCCACCTTAC
F1	CAACATACGAGCCGGAAGCATAAAGTG
F2	CATCTTCGGCAACGTGTCCGCCATC
R'	GGAAACCTGCTCCTCCCAATTCCGTCC

sc, genotype primers used for screening target ES clones; F, forward; R, reverse; probe-F/R, primers used for amplifying the 3'probe.

protein was loaded per lane. Denatured protein samples were separated by 10% SDS-PAGE and transferred to a PVDF membrane (Bio-Rad Laboratories, Inc.). Then the membranes were blocked with 5% milk powder for 1 h at room temperature. Primary antibodies diluted in 5% BSA were used to probe the targeted proteins for 18 h at 4°C. The corresponding secondary antibody was used to enhance the signal for 1 h at room temperature. Finally, the blot bands were visualized using enhanced chemiluminescence (Pierce, Thermo Scientific). Details of antibodies are given in Table SII. ImageJ fiji software (version v1.53c; National Institutes of Health) was used for densitometric analysis.

Co-immunoprecipitation. Proteins were extracted from 100 mg of tissue using 1 ml of ice-cold RIPA lysis buffer containing fresh protease and phosphatase inhibitors (Beyotime Institute of Biotechnology; cat. no. P0013D) and concentrations measured. After treatment of samples, 500 µg of proteins diluted in 500 µl of RIPA lysis buffer were incubated with primary antibody (Integrin β1: 2 µg per IP reaction; KCNH2: 2 µg per IP reaction) and goat IgG isotype control (2 µg per IP reaction) separately, and then with rotation overnight at 4°C. Magnetic beads (Beyotime Institute of Biotechnology; cat. no. P2105) were added and the mixture was shaken for another 4 h. After incubation, the mixtures were placed on a magnetic stand (Invitrogen; Thermo Fisher Scientific, Inc.) for 10 sec at 4°C to separate the beads. The bead complexes were washed with RIPA lysis buffer and then the immunoprecipitants were mixed with SDS loading buffer, boiled for 10 min and subjected to western blotting as aforementioned (see Table SII for details of antibodies).

Terminal deoxynucleotidyl transferase (TdT)-mediated dUTP nick end labelling (TUNEL) assay. Apoptosis of rat embryos was detected by TUNEL assay (Roche Diagnostics GmbH). After fixation and permeabilization, TUNEL reaction mixture was added to each sample and the samples were incubated for 1 h at 37°C in dark. After adding Hoechst (cat. no. 14530-100MG; MilliporeSigma) and incubating the samples for 12 min at room temperature in the dark, the cells were rinsed with PBS and imaged with a Leica confocal microscope (Leica Microsystems GmbH). The normalized

results were determined by comparing the TUNEL-positive (red) cells to the total nuclei in 3-6 randomly chosen microscopic fields.

Data access. The EGAS00001003996 dataset in the European Genome-phenome Archive (EGA) contains human embryonic heart small conditional RNA (sc)RNA-seq data of 6.5-7 weeks post-conception, including a total of 3,717 single-cells as determined by 10X Genomics (21).

Identification of cell types. Dimensionality reduction and clustering of the scRNA-seq data were performed using the Seurat package (version 4.1.1) of R (version 4.3.1; <http://www.R-project.org/>). The highly variable genes were selected using the FindVariableGenes function and clusters were identified using the FindClusters function with the same settings as previously reported (21). Different cell types were identified based on the abundance of cell clusters and the cardiac function represented by the cardiomyocyte clusters according to known marker genes. Uniform manifold approximation and projection (UMAP) was used to visualize single-cells.

Trajectory analysis. The pseudotime trajectories of ventricular cardiomyocytes were constructed using the dynverse dyno (version 0.1.2) set of R packages for trajectory inference (TI) with single-cell data (22). Single cell matrices were extracted from the Seurat object and wrapped into a dynwrap object using dynwrap wrap_expression. Then the immature cardiomyocytes, trabecular cardiomyocytes, inner compact zone (ICZ) cardiomyocytes and outer compact zone (OCZ) cardiomyocytes were respectively imported into a multiple spanning tree (MST). Pseudotime visualization was obtained using calculated pseudotimes on the MST model object.

Statistical analysis. Statistical analyses were performed using GraphPad Prism V software (GraphPad Software; Dotmatics). All assays were repeated independently at least three times. The data are represented as mean ± SD in the figures. Differences between the two groups were compared using unpaired Student's t-test. Differences between three or more groups were compared using one-way ANOVA with Tukey's post hoc test. P<0.05 was considered to indicate a statistically significant difference.

Results

Generation of *Kcnh2* gene knockout rats. Exons 7 and 8 of the rat *Kcnh2* gene encode the pore region of the ether-a-go-go protein. To delete exons 7 and 8, the targeting vector was introduced into DAC8 rat ESCs via electroporation. After the recombination reaction, exons 7 and 8 were replaced with the positive selection cassette CAG-EGFP-IRES-Pac (Fig. 1A). For genotyping, the targeted rESCs were confirmed by PCR and Southern blot (Fig. 1B and C) and then expanded and microinjected into E4.5 Fisher344 blastocysts. Thereafter, the rESC-injected blastocysts were transferred into pseudo-pregnant SD rats. Male chimaeras (Fig. S1) were cross-bred with WT SD female rats to generate germline pups (Fig. 1D). Germline transmission of the *Kcnh2* mutant allele was then

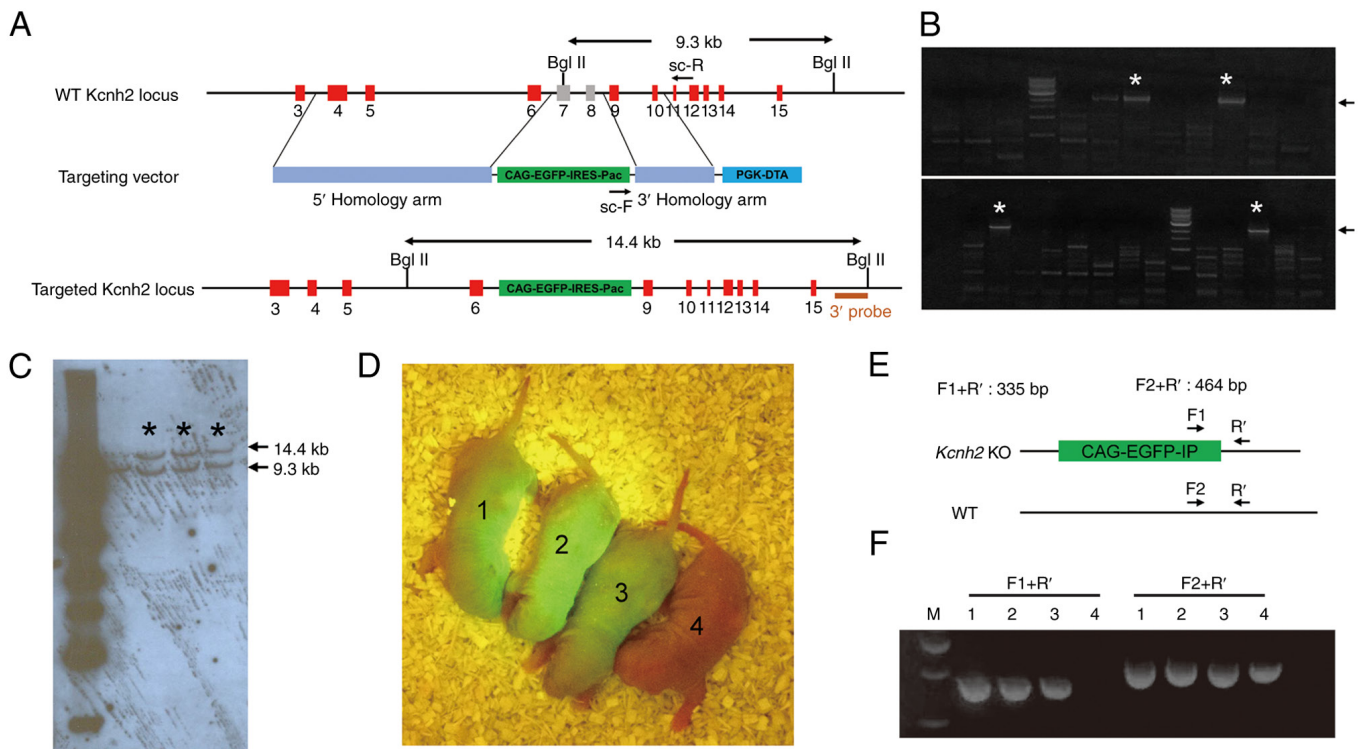


Figure 1. Generation of *Kcnh2* mutant rats by homologous recombination. (A) Schematic diagram showing the WT allele of rat *Kcnh2* gene, the *Kcnh2* targeting vector and the targeted *Kcnh2* gene locus. (B) PCR screening results for drug-resistant clones using the primers shown in (A). The expected product of 2.6 kb is indicated by an arrow. The asterisks indicate the clones picked for the next step. (C) Southern blot analysis for *Kcnh2* gene-targeted ES cells in the selected 4 clones from (B). The genomic DNA was digested by *Bgl*II and the 3'probe indicated in (A) was used for blotting. Among the four rESCs clones, three of them were correctly targeted as indicated by the asterisks. (D) Germline pups were generated by crossing the male chimaera with a WT Sprague-Dawley female rat. The expression of GFP signified that the targeted allele was transmitted to the pups. (E) Diagrams showing the positions of three PCR primers designed to genotype *Kcnh2* targeted pups. (F) Genotyping results of germline pups from (E). All GFP-positive pups generated two bands, which indicates that all of them are heterozygous and the *Kcnh2* targeted allele was transmitted. All primer sequences are shown in Table I. sc-F/sc-R, genotype primers used for screening target ES clones; 3'probe used for southern blotting; F1/F2/R', primers used for genotype of rats; M, DNA marker.

verified based on the EGFP expression of F1 offspring and PCR genotyping (Fig. 1E and F). *Kcnh2* heterozygous germline rats showed a normal growth rate and body weight and were fertile.

***Kcnh2* depletion leads to developmental defects.** Mendelian ratios were counted for the hybrid offspring after crossing of heterozygous mutant rats (Table SIII). To our surprise, homozygous offspring were not found, which suggested that the *Kcnh2*^{-/-} genotype might induce embryonic lethality. To determine when the embryos stopped developing in the early stage, *Kcnh2*^{-/-} embryos were dissected at different time points during pregnancy. Prior to E10.5, no obvious differences were observed in body size at matched stages of development (Fig. 2A). After E10.5, the *Kcnh2*^{-/-} embryos developed slowly, showing a smaller body size. By E15.0, however, no live *Kcnh2*^{-/-} embryos were found (Fig. S2). Moreover, *Kcnh2*^{-/-} embryos at E11.0 exhibited with a massive pericardial effusion, which was very likely a consequence of heart failure with evidence of structural deformity in the bulbus cordis right ventricle and the outflow tract (Fig. 2B). Additionally, a reduction in myocardial thickness in embryonic hearts and dilation of the first branchial arch artery were identified and the length and structure of myofibrils were greatly affected (Fig. 2C). By contrast, *Kcnh2*^{+/-} embryos showed embryonic conformations similar to those of WT embryos.

In *Kcnh2*^{-/-} rats, no shorter variant blots were detected (Fig. S3), suggesting the channel protein was knocked out (13). To determine the potential role of KCNH2 in normal development, the KCNH2 expression status was assessed at different stages (Fig. 2D and E). KCNH2 expression gradually increased beginning at E10, peaked at E15 and then decreased progressively during later embryonic stages and the postnatal period. The distribution of KCNH2 at E10.5 was found to be very different, especially in cardiomyocytes (Fig. 2F), which was further verified by an expression assay of different embryonic tissues (Fig. 2G and H). In *Kcnh2*^{-/-} embryos at E10.5, the markers of angiogenesis and nervous system development were not significantly altered (Figs. S4 and 2I), while the expression of the related genes of both the first heart field, such as HCN4 and TBX5 and the second heart field, including MEF2C, ISL1 and Hand2, were significantly decreased (Fig. S5). These findings were consistent with the expression patterns of E11 embryos (Fig. 2J), indicating an abnormal status in the embryonic heart. In addition, to explore the influence of KCNH2 channel activity on embryonic and heart development, E4031, a pharmacological blocker of Kv11.1 ion-conducting properties was used to treat pregnant rats. The embryos treated with E4031 for 2 or 3 days after E9.5 showed abnormal phenotypes, similar to those of *Kcnh2*^{-/-} rats, such as significantly reduced body and heart sizes (Fig. S6A-C). Moreover, inhibition of KCNH2 at E10.5 or E11.5 caused embryonic lethality

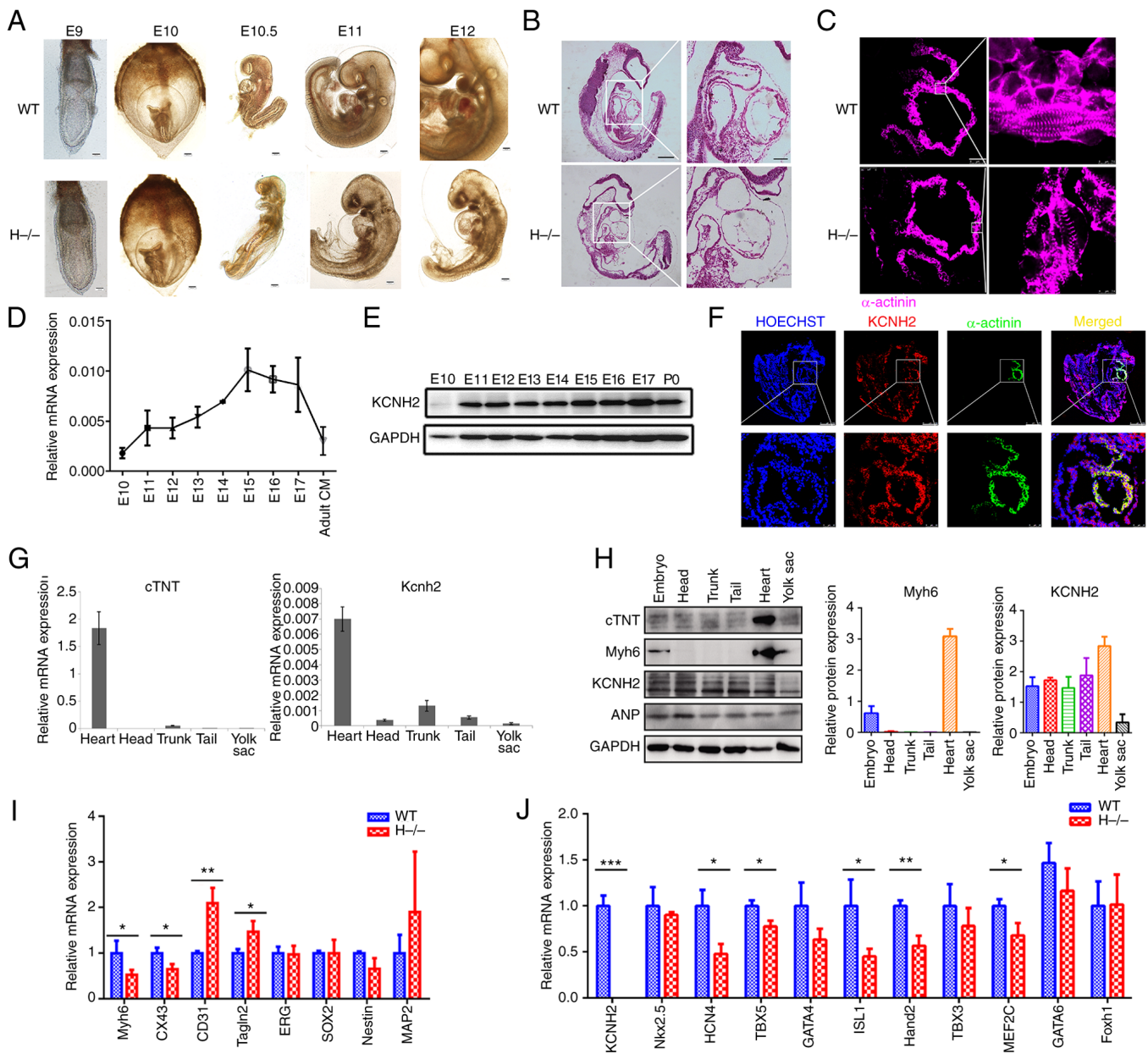


Figure 2. Developmental status of *Kcnh2* knockout rat embryos. (A) Comparison of embryo growth characteristics of WT- and *Kcnh2* knockout rats. Rat embryos were dissected at E9, E10, E10.5, E11 and E12 (scale bar, 250 μ m). (B) Histological analysis of both WT and *Kcnh2* knockout rats at E11. Massive pericardial effusion was observed in *Kcnh2* knockout rats (whole embryo scale bar, 250 μ m, embryonic heart scale bar, 50 μ m). (C) Immunofluorescence images showing the size and structure of the myofibrils of *Kcnh2*^{-/-} E11 embryos (scale bar, 50 μ m). Expression of KCNH2 in the whole embryo during embryonic development stages as assayed by (D) RT-qPCR and (E) western blotting. (F) Distribution of KCNH2 at E10.5, especially in the heart (scale bar, 50 μ m). Expression of KCNH2 in different tissues at E10.5 assayed by (G) RT-qPCR and (H) western blotting. (I) Expression status of cardiac, angiogenesis and nervous system development markers at E10.5 heart tissue. (J) RT-qPCR analysis of cardiac markers of *Kcnh2* knockout rats at E11 heart tissue. Data are represented as mean \pm SD (n=3), (*P<0.05, **P<0.01, ***P<0.005, vs. WT). WT, wild-type; RT-qPCR, reverse transcription-quantitative PCR.

(Fig. S6D and E), which partly recapitulated the *Kcnh2* knockout phenotype. Therefore, the activity of KCNH2 is essential for maintaining early embryonic development in rats.

KCNH2 is associated with compact cardiomyocyte development during the early embryonic stage. During the early stage of embryonic development, trabecular cardiomyocytes are first to develop, followed by compact cardiomyocytes, which promote the thickening of the myocardium (23). KCNH2 affected the process *in vivo* (Fig. 2B and C) and has been found to mediate the differentiation of rESCs into

cardiomyocytes *in vitro* (13), but the mechanism underlying the arrest of embryonic development in the absence of KCNH2 is unclear. To understand whether the distribution of KCNH2 in different types of cardiomyocytes is related to the formation of the compact myocardium, human embryonic hearts of 6.5-7 weeks post-conception and further subpopulations of the cardiomyocyte population were analyzed (21). According to the expression status of marker genes (Fig. 3A), eight clusters of the cells were classified, including both ICZ and OCZ cardiomyocytes, trabecular cardiomyocytes, atrial cardiomyocytes, cardiac conduction system (CCS) cardiomyocytes,

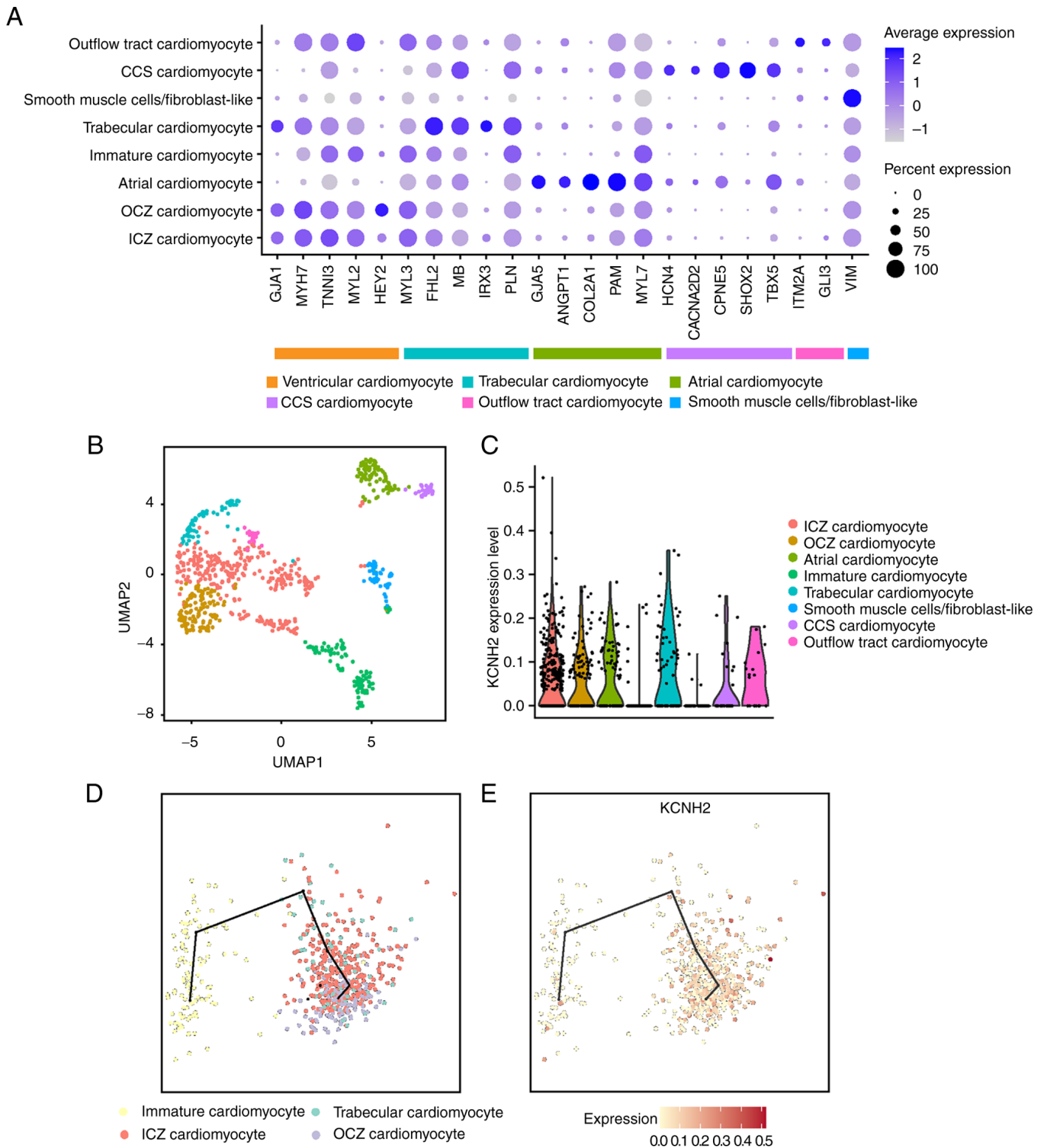


Figure 3. Distribution and expression features of *KCNH2* in human embryonic heart at 6.5-7 weeks post-conception. (A) Bubble plots showing the expression levels of known marker genes for each cell population. (B) UMAP visualization of cardiomyocyte clusters from the human embryonic heart of 6.5-7 weeks post-conception. (C) Violin plots showing the expression levels of *KCNH2* in different cardiomyocyte clusters. (D) Pseudotemporal trajectory of cardiomyocyte clusters constructed by multiple spanning tree. (E) Expression of *KCNH2* along the trajectory. *KCNH2*, potassium voltage-gated channel subfamily H member 2; UMAP, uniform manifold approximation and projection.

outflow tract cardiomyocytes, immature cardiomyocytes and finally a cluster of smooth muscle cell/fibroblast-like cells. These clusters were combined and visualized through UMAP concerning cell identity (Fig. 3A and B). The analysis of the present study indicated that *KCNH2* was expressed in compact cardiomyocytes, trabecular cardiomyocytes, atrial

cardiomyocytes, CCS cardiomyocytes and outflow tract cardiomyocytes (Fig. S7A), but not in immature cardiomyocytes (Fig. 3C). To determine the progressive development of compact cardiomyocytes during the maturation process, a pseudotime analysis on ventricular cardiomyocytes based on ventricle-specific markers was performed to construct the

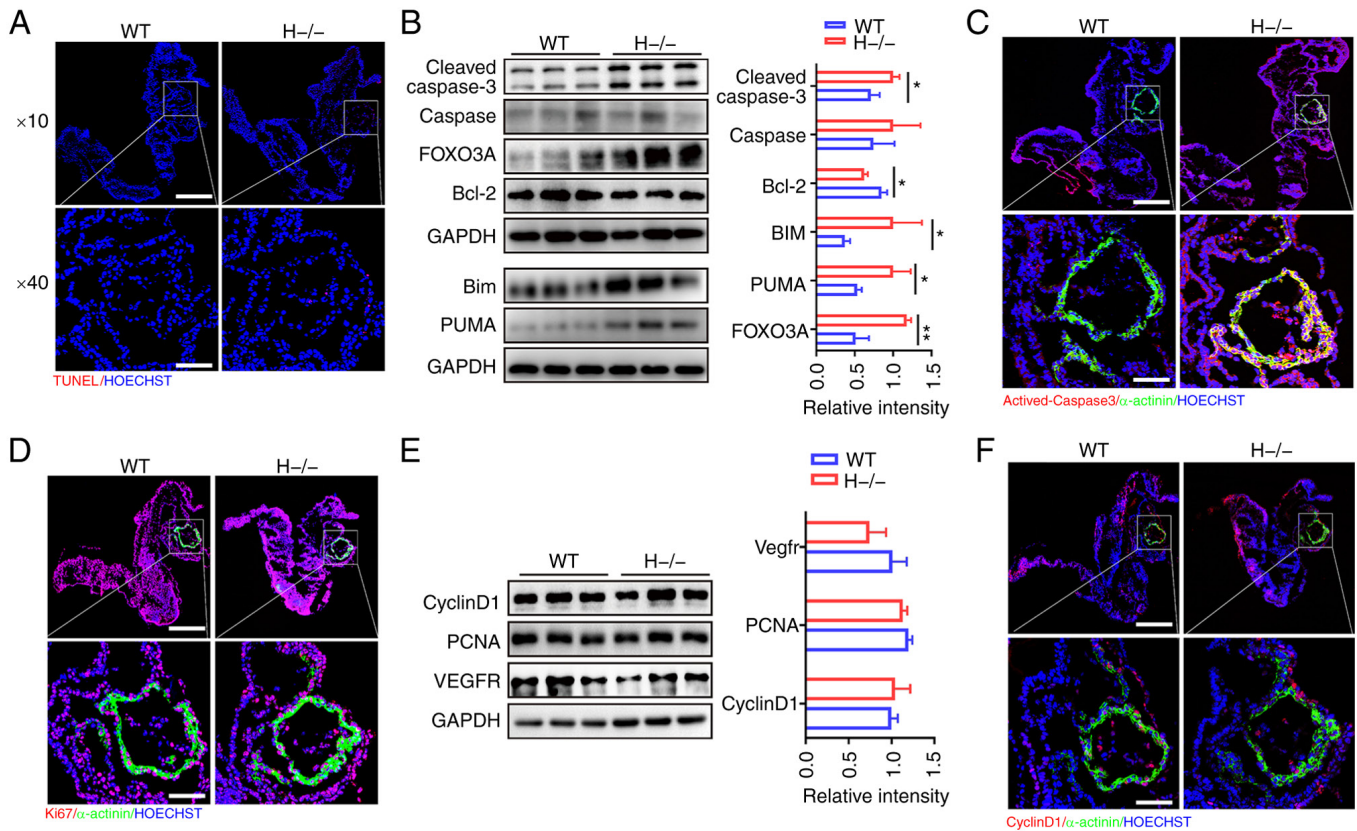


Figure 4. Knockout of *Kcnh2* induces massive cardiac apoptosis at the embryonic stage. (A) TUNEL assay for extensive apoptosis in E10.5 *Kcnh2* knockout rat embryos. (B and C) Western blot and immunofluorescence staining for apoptosis-related markers in E10.5 WT and *Kcnh2* knockout rat embryos. (D) Immunofluorescence image of Ki67 with α -actinin in *Kcnh2* knockout rat embryos at E10.5. (E and F) Western blot and immunofluorescence analysis of the changes in proliferation-related genes in E10.5 embryos. Data are represented as mean \pm SD (n=3), *P<0.05, **P<0.01, ***P<0.005, vs. WT; scale bar, 50 μ m. WT, wild-type; FOXO3A, forkhead box O3A; Bim, Bcl-2 like 11; PUMA, p53 upregulated modulator of apoptosis; PCNA, proliferating cell nuclear antigen.

trajectory of cardiomyocytes development. In this process, the pseudotime trajectory began with immature cardiomyocytes, moved to trabecular cardiomyocytes and ICZ cardiomyocytes and gradually progressing to OCZ cardiomyocytes (Fig. 3D). It was found that KCNH2 was upregulated along the trajectory (Fig. 3E), similar to the case for the maturation markers, creatine kinase-mitochondrial 2 and myosin heavy chain 7 (Fig. S7B and C). These results matured with the expression trend during early embryonic development (Fig. 4D) and suggested that KCNH2 might play a crucial role in the differentiation of compact cardiomyocytes involved in heart development.

Kcnh2 depletion induces embryonic apoptosis rather than inhibiting proliferation. KCNH2 has been shown to regulate apoptosis and proliferation to control cell fate *in vitro* (4). Although a previous study has shown that homozygous missense N629D *Kcnh2* potassium channel mutation causes developmental defects in the right ventricle, outflow tract and embryonic lethality (24), the mechanism in embryonic development has not yet been confirmed. The immunostaining TUNEL assay showed that the apoptosis of *Kcnh2*^{-/-} embryos increased significantly (Fig. 4A). Consistently, the *Kcnh2* mutation increased the cleaved caspase3/caspase3 ratio and enhanced the expression of the proapoptosis-related genes Bcl-2 like 11 (Bim) and p53 upregulated modulator of apoptosis (PUMA; Fig. 4B and C). FOXO3A, which can

transcriptionally increase the expression of Bim and regulate embryo cell fate (25), was also upregulated. However, the proliferation marker Ki67 did not display any change at E10.5 embryos in the absence of KCNH2 (Fig. 4D). Furthermore, the expression of proliferation-related genes such as cyclin D1, proliferating cell nuclear antigen (PCNA) and VEGFR remained unchanged (Fig. 4E and F). These results suggested that KCNH2 is necessary to prevent apoptosis during embryo development.

KCNH2 interacts with integrin β 1 to modulate the activity of AKT. Our previous findings have demonstrated that KCNH2 interacts with integrin β 1 to activate the AKT signaling pathway during the differentiation of rESCs into cardiomyocytes (13). However, the relationship between the KCNH2/integrin β 1 complex and the AKT pathway has not yet been confirmed *in vivo*. To explore how KCNH2 is involved in FOXO3A regulation, it was next assessed whether KCNH2 associates with integrin β 1 to modulate AKT activity by mediating the phosphorylation of FAK (26). Immunofluorescence staining of E10.5 WT embryos showed relatively high expression of integrin β 1, which was distributed along the cell membrane (Fig. 5A). Immunoprecipitation further confirmed that KCNH2 indeed interacted with integrin β 1 (Fig. 5B). In addition, the integrin β 1 protein, but not its mRNA (Fig. S8), was downregulated in *Kcnh2* knockout embryos (Fig. 5C and D), suggesting that KCNH2 might play a role in the stability of

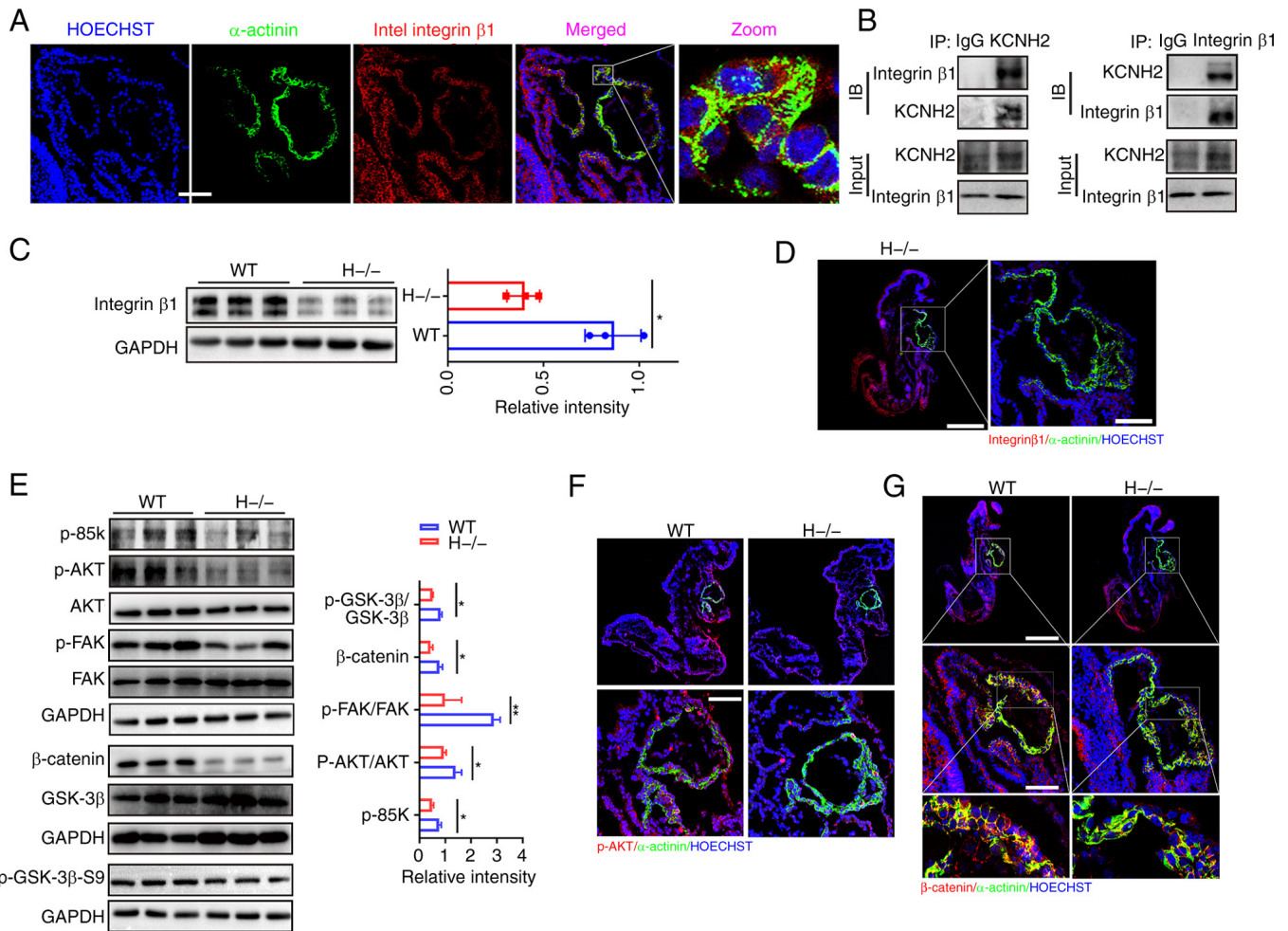


Figure 5. KCNH2 interacts with integrin $\beta 1$ to modulate apoptosis during embryonic development. (A) Distribution of integrin $\beta 1$ in WT rats at E10.5 as revealed by immunofluorescence assay. (B) Co-immunoprecipitation assay for the interaction of KCNH2 with integrin $\beta 1$ in WT rat embryos at E10.5. (C) Western blotting showing the decreased expression of integrin $\beta 1$ in *Kcnh2*^{-/-} rat embryos (compared with the merged image in 5A). (D) Immunofluorescence images showing integrin $\beta 1$ expression status in *Kcnh2*^{-/-} rat embryos (compared with the merged image in 5A). (E) Western blot or (F and G) immunofluorescence images showing the expression status of p-AKT, p-FAK, β -catenin and p-GSK-3 β -S9 in E10.5 embryos of *Kcnh2*^{-/-} rats. Data are represented as mean \pm SD (n=3), *P<0.05, **P<0.01, ***P<0.005 vs. WT; scale bar, 50 μ m. KCNH2, potassium voltage-gated channel subfamily H member 2; WT, wild-type; p-, phosphorylated; FAK, focal adhesion kinase; GSK, glycogen synthase kinase.

integrin $\beta 1$ rather than affecting its transcriptional expression. Consistent with the disruption of integrin $\beta 1$ with KCNH2, the phosphorylation of FAK was also decreased in *Kcnh2* depleted rats, which then induced a decrease in AKT activity (Fig. 5E and F). The reduction of AKT activity with this genotype also triggered increases in p-GSK-3 β -S9 (Fig. 5E) and calcium/calmodulin dependent protein kinase II (CaMKII) (Fig. S9) levels, but a decrease in β -catenin at E10.5 embryos (Fig. 5E and G). Taken together, these results suggest that KCNH2 can directly interact with integrin $\beta 1$ to facilitate the phosphorylation of AKT to prevent apoptosis in the rat heart during embryonic development.

Discussion

Homozygous depletion of *Kcnh2* in rats can impair the early heart development process in rats. Consistent with previous reports (27,28), the present study found that the expression of KCNH2 begins at E10.0, peaks at the E15 developmental stage and thereafter maintains relatively low. Similar to the N629D

mutant of *Kcnh2* in mice, which has been proven to induce defects mainly in the second heart field (SHF) (24), the results of the present study also revealed general dysfunction of the embryonic heart, including in the SHF. In addition, the failure to distribute KCNH2 in compact cardiomyocytes might have induced heart defects during the embryonic stage. In addition, *Kcnh2* depletion downregulated the related genes participating in cardiac development and/or adult heart function in embryos or embryonic cardiomyocytes, indicating a crucial role of KCNH2 in early heart development.

KCNH2 has been shown to modulate cell fate by controlling cell proliferation and apoptosis (4). The present study demonstrated that KCNH2 depletion in rat embryos led to apoptosis but not proliferation, especially in the embryonic heart. In addition, excessive activation of CaMKII was detected in *Kcnh2* knockout embryos, which might be associated with a variety of heart diseases involving in cardiomyocyte apoptosis (29).

Integrin $\beta 1$ is a heterodimeric molecule that mediates cell adhesion due to its affinity for the extracellular matrix, which is critical for the developmental processes (30). Notably, CaMKII

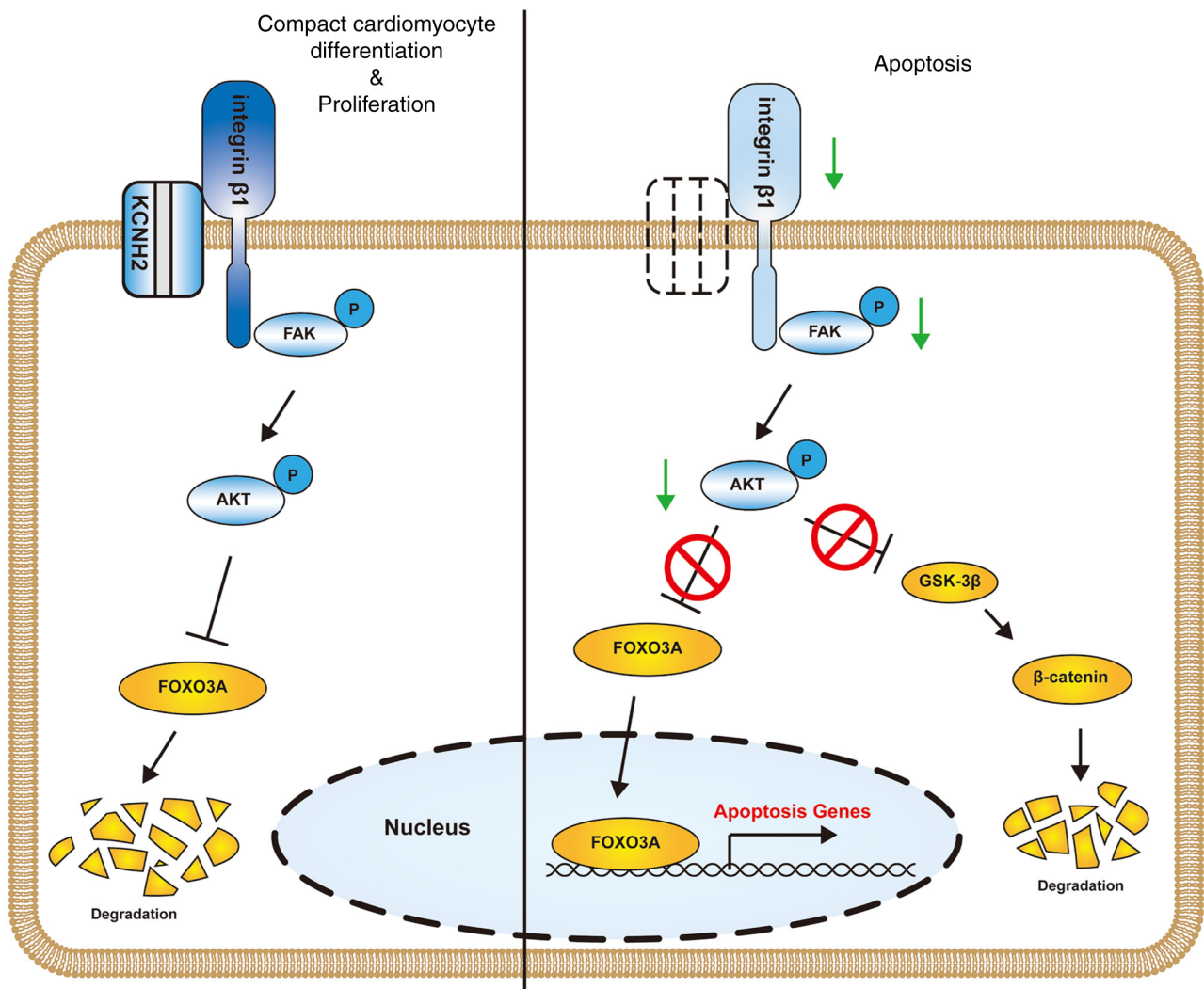


Figure 6. Working model of apoptosis induced by KCNH2 deficiency. KCNH2 and Integrin $\beta 1$ form a complex that mediates the Akt/GSK-3 β / β -catenin and Akt/FOXO3A signaling pathways, which maintain the normal development of the heart. KCNH2, potassium voltage-gated channel subfamily H member 2; FAK, focal adhesion kinase; GSK, glycogen synthase kinase; FOXO3A, forkhead box O3A.

can inhibit the function of integrin $\beta 1$ by regulating integrin cytoplasmic domain-associated protein-1 α (ICAP1 α) (31). The present study confirmed that KCNH2 interacts with integrin $\beta 1$ to regulate the phosphorylation level of FAK, which is one of the fundamental molecules in integrin-dependent pathways (26). FAK is normally recruited into newly-formed focal adhesions, through autophosphorylation to affect multiple cellular processes, including cell survival, proliferation and differentiation, by modulating the activity of downstream effectors such as PI3K and AKT (32,33). The present study revealed that disruption of the KCNH2/integrin $\beta 1$ complex affected the expression of integrin $\beta 1$ at the protein but not at the transcriptional level. These findings suggested that KCNH2 might maintain the stability of integrin $\beta 1$ via association with it. Furthermore, deletion of KCNH2 weakened the activity of FAK and AKT. These findings suggested that the early developmental impairment observed in *Kcnh2* knockout homozygotes may be mediated through the FAK/AKT pathways. Given that integrin $\beta 1$ regulates cardiomyocyte apoptosis, overexpression of FAK could enable cardiomyocytes to become more resistant to apoptosis. In addition, inhibition of KCNH2 disassociates

with FAK, which is then cleaved, resulting in activation of the FAK-dependent apoptosis pathway (34). Thus, KCNH2 associate with $\beta 1$ integrin to sustain FAK activity for normal cardiac development.

FOXO transcriptional activity can be regulated by a variety of signaling pathways, including PI3K-mediated activation of AKT, which directly phosphorylates FOXO at serine 256, leading to its nuclear export and thereby inactivation. In the absence of negative regulation of AKT, FOXO factors generally remain in the nucleus and induce transcription of a variety of downstream target genes that collectively inhibit proliferation and induce cell cycle withdrawal. In the present study, knockout of *Kcnh2* in rats resulted in an increase of FOXO3a expression, which transcriptionally activated the proapoptotic genes Bim and PUMA. Notably, the present study also found that the loss of KCNH2 increased the expression of CaMKII, thus, a sustained CaMKII phosphorylation may promote apoptosis.

Although the *Kcnh2*^{-/-} genotype induced embryonic lethality, the heterozygous rats survived. The electrophysiological studies showed that *Kcnh2*^{+/-} cardiomyocytes of newborn rats displayed currents similar to those of WT rats (Fig. S10). Similarly, normal

heart structural variables in *Kcnh2*^{+/-} and WT cardiomyocytes, including the left ventricular posterior wall, interventricular septal thickness and left ventricular internal diameter (Fig. S11), were observed. However, the 1-4 month-old *Kcnh2*^{+/-} rats displayed a typical prolonged QTc phenotype (15) and an increase in the T wave interval (Fig. S12A). When these mutant rats were treated with propranolol, the abnormal electrophysiological were completely eliminated (Fig. S12B). The previous mouse model with *Kcnh2* deletion displayed only a reduction of repolarization current, without QT prolongation (35,36). The present results suggested that the *Kcnh2*^{+/-} rat model was more suitable than the *Kcnh2*^{+/-} mouse model for elucidating the detailed mechanisms of cardiac arrhythmia.

In conclusion, homozygous *Kcnh2* knockout in rats resulted in an arrest of embryonic development due to the absence of KCNH2 distribution in compact cardiomyocytes, which then induced apoptosis via failure of KCNH2 to form complexes with integrin β 1 (Fig. 6). These results suggested that KCNH2, in addition to being a classical potassium channel that conducts current for action potentials in cardiomyocytes, plays a check-point role in rat embryonic development.

Acknowledgements

The authors thank Dr Hailin Zhang from Hebei Medical University and Dr Takako Makita from Medical University of South Carolina for some of electrophysiological experiments.

Funding

The present study was supported by the National Natural Science Foundation of China (grant nos. 32071109, 82070270, 81870242 and M-0048), the Shanghai Committee of Science and Technology (grant nos. 22ZR1463800 and 21ZR1467000) and CAMS Innovation Fund for Medical Sciences (grant ns. 2019-I2M-5-053).

Availability of data and materials

The datasets used and/or analyzed during the current study are available from the corresponding author on reasonable request.

Authors' contributions

SHu and ZL were responsible for data curation, formal analysis, investigation, methodology and writing the original draft of the manuscript. HL, WC, YM and CL were responsible for methodology and formal analysis. SHe, QL and MS were responsible for software and visualization. FL, NY, HW, AS and QY were responsible for methodology. LL and LP were responsible for conceptualization, supervision, writing, reviewing and editing. LP, LL and SHu confirm the authenticity of all the raw data. All authors read and approved the final manuscript.

Ethics approval and consent to participate

All of the procedures were approved by Institutional Animal Care and Use Committee at Tongji University (approval no. TJLAC-016-022).

Patient consent for publication

Not applicable.

Competing interests

The authors declare that they have no competing interests.

Authors' information

LL is a Fellow at the Collaborative Innovation Center For Cardiovascular Disease Translational Medicine, Nanjing Medical University.

References

- Warmke JW and Ganetzky B: A family of potassium channel genes related to eag in Drosophila and mammals. *Proc Natl Acad Sci USA* 91: 3438-3442, 1994.
- Sanguinetti MC, Jiang C, Curran ME and Keating MT: A mechanistic link between an inherited and an acquired cardiac arrhythmia: HERG encodes the IKr potassium channel. *Cell* 81: 299-307, 1995.
- Sanguinetti MC and Tristani-Firouzi M: hERG potassium channels and cardiac arrhythmia. *Nature* 440: 463-469, 2006.
- Jehle J, Schweizer PA, Katus HA and Thomas D: Novel roles for hERG K(+) channels in cell proliferation and apoptosis. *Cell Death Dis* 2: e193, 2011.
- Bhuiyan ZA, Momenah TS, Gong Q, Amin AS, Ghamdi SA, Carvalho JS, Homfray T, Mannens MM, Zhou Z and Wilde AA: Recurrent intrauterine fetal loss due to near absence of HERG: Clinical and functional characterization of a homozygous nonsense HERG Q1070X mutation. *Heart Rhythm* 5: 553-561, 2008.
- Klaver EC, Versluijs GM and Wilders R: Cardiac ion channel mutations in the sudden infant death syndrome. *Int J Cardiol* 152: 162-170, 2011.
- Pillozzi S, Brizzi MF, Bernabei PA, Bartolozzi B, Caporale R, Basile V, Boddi V, Pegoraro L, Becchetti A and Arcangeli A: VEGFR-1 (FLT-1), β 1 integrin and hERG K+ channel for a macromolecular signalling complex in acute myeloid leukemia: Role in cell migration and clinical outcome. *Blood* 110: 1238-1250, 2007.
- Broders-Bondon F, Paul-Gilloteaux P, Carlier C, Radice GL and Dufour S: N-cadherin and beta1-integrins cooperate during the development of the enteric nervous system. *Dev Biol* 364: 178-191, 2012.
- Becchetti A, Crescioli S, Zanieri F, Petroni G, Mercatelli R, Coppola S, Gasparoli L, D'Amico M, Pillozzi S, Crociani O, *et al.*: The conformational state of hERG1 channels determines integrin association, downstream signalling and cancer progression. *Sci Signal* 10: eaaf3236, 2017.
- Gonzalez-Juanatey JR, Iglesias MJ, Alcaide C, Pineiro R and Lago F: Doxazosin induces apoptosis in cardiomyocytes cultured in vitro by a mechanism that is independent of alpha1-adrenergic blockade. *Circulation* 107: 127-131, 2003.
- Staudacher I, Jehle J, Staudacher K, Pledl HW, Lemke D, Schweizer PA, Becker R, Katus HA and Thomas D: HERG K+ channel-dependent apoptosis and cell cycle arrest in human glioblastoma cells. *PLoS One* 9: e88164, 2014.
- Afrasiabi E, Hietamaki M, Viitanen T, Sukumaran P, Bergelin N and Tornquist K: Expression and significance of HERG (KCNH2) potassium channels in the regulation of MDA-MB-435S melanoma cell proliferation and migration. *Cell Signal* 22: 57-64, 2010.
- Wang D, Liu C, Liu H, Meng Y, Lin F, Gu Y, Wang H, Shang M, Tong C, Sachinidis A, *et al.*: ERG1 plays an essential role in rat cardiomyocyte fate decision by mediating AKT signalling. *Stem Cells* 39: 443-457, 2021.
- Abeyathna P and Su Y: The critical role of Akt in cardiovascular function. *Vasc Pharmacol* 74: 38-48, 2015.
- Li Z, Meng Y, Liu C, Liu H, Cao W, Tong C, Lu M, Li L and Peng L: *Kcnh2* mediates FAK/AKT-FOXO3A pathway to attenuate sepsis-induced cardiac dysfunction. *Cell Proliferat* 54: e12962, 2021.

16. Li P, Tong C, Mehriani-Shai R, Jia L, Wu N, Yan Y, Maxson RE, Schulze EN, Song H, Hsieh CL, *et al*: Germline competent embryonic stem cells derived from rat blastocysts. *Cell* 135: 1299-1310, 2008.
17. Tong C, Li P, Wu NL, Yan Y and Ying QL: Production of p53 gene knockout rats by homologous recombination in embryonic stem cells. *Nature* 467: 211-213, 2010.
18. Tong C, Huang G, Ashton C, Li P and Ying QL: Generating gene knockout rats by homologous recombination in embryonic stem cells. *Nat Protoc* 6: 827-844, 2011.
19. Ying QL, Wray J, Nichols J, Battle-Morera L, Doble B, Woodgett J, Cohen P and Smith A: The ground state of embryonic stem cell self-renewal. *Nature* 453: 519-523, 2008.
20. Livak KJ and Schmittgen TD: Analysis of relative gene expression data using real-time quantitative PCR and the 2(-Delta Delta C(T)) method. *Methods* 25: 402-408, 2001.
21. Asp M, Giacomello S, Larsson L, Wu C, Fürth D, Qian X, Wårdell E, Custodio J, Reimegård J, Salmén F, *et al*: A Spatiotemporal Organ-wide gene expression and cell atlas of the developing human heart. *Cell* 179: 1647-1660, 2019.
22. Saelens W, Cannoodt R, Todorov H and Saey Y: A comparison of single-cell trajectory inference methods. *Nat Biotechnol* 37: 547-554, 2019.
23. Funakoshi S, Fernandes I, Mastikhina O, Wilkinson D, Tran T, Dhahri W, Mazine A, Yang D, Burnett B, Lee J, *et al*: Generation of mature compact ventricular cardiomyocytes from human pluripotent stem cells. *Nat Commun* 12: 3155, 2021.
24. Teng GQ, Zhao X, Lees-Miller JP, Quinn FR, Li P, Rancourt DE, London B, Cross JC and Duff HJ: Homozygous missense N629D hERG (KCNH2) potassium channel mutation causes developmental defects in the right ventricle and its outflow tract and embryonic lethality. *Circ Res* 103: 1483-1491, 2008.
25. Evans-Anderson HJ, Alfieri CM and Yutzey KE: Regulation of cardiomyocyte proliferation and myocardial growth during development by FOXO transcription factors. *Circ Res* 102: 686-694, 2008.
26. Becchetti A, Petroni G and Arcangeli A: Ion channel conformations regulate integrin-dependent signalling. *Trends Cell Biol* 29: 298-307, 2019.
27. Franco D, Demolombe S, Kupersmidt S, Dumaine R, Dominguez JN, Roden D, Antzelevitch C, Escande D and Moorman AF: Divergent expression of delayed rectifier K(+) channel subunits during mouse heart development. *Cardiovasc Res* 52: 65-75, 2001.
28. Wang H, Zhang Y, Cao L, Han H, Wang J, Yang B, Nattel S and Wang Z: HERG K+ channel, a regulator of tumor cell apoptosis and proliferation. *Cancer Res* 62: 4843-4848, 2002.
29. Feng N and Anderson ME: CaMKII is a nodal signal for multiple programmed cell death pathways in heart. *J Mol Cell Cardiol* 103: 102-109, 2017.
30. Lei L, Liu D, Huang Y, Jovin I, Shai SY, Kyriakides T, Ross RS and Giordano FJ: Endothelial expression of beta1 integrin is required for embryonic vascular patterning and postnatal vascular remodeling. *Mol Cell Biol* 28: 794-802, 2008.
31. Millon-Fremillon A, Brunner M, Abed N, Collomb E, Ribba AS, Block MR, Albiges-Rizo C and Bouvard D: Calcium and calmodulin-dependent serine/threonine protein kinase type II (CaMKII)-mediated intramolecular opening of integrin cytoplasmic domain-associated protein-1 (ICAP-1alpha) negatively regulates beta1 integrins. *J Biol Chem* 288: 20248-20260, 2013.
32. Frame MC, Patel H, Serrels B, Lietha D and Eck MJ: The FERM domain: Organizing the structure and function of FAK. *Nat Rev Mol Cell Bio* 11: 802-814, 2010.
33. Torsoni AS, Constancio SS, Nadruz WJ, Hanks SK and Franchini KG: Focal adhesion kinase is activated and mediates the early hypertrophic response to stretch in cardiac myocytes. *Circ Res* 93: 140-147, 2003.
34. He S, Moutaoufik MT, Islam S, Persad A, Wu A, Aly KA, Fonge H, Babu M and Cayabyab FS: HERG channel and cancer: A mechanistic review of carcinogenic processes and therapeutic potential. *Biochim Biophys Acta Rev Cancer* 1873: 188355, 2020.
35. Lees-Miller JP, Guo J, Somers JR, Roach DE, Sheldon RS, Rancourt DE and Duff HJ: Selective knockout of mouse ERG1 B potassium channel eliminates I(Kr) in adult ventricular myocytes and elicits episodes of abrupt sinus bradycardia. *Mol Cell Biol* 23: 1856-1862, 2003.
36. Roden DM: Clinical practice. Long-QT syndrome. *New Engl J Med* 358: 169-176, 2008.



Copyright © 2023 Hu et al. This work is licensed under a Creative Commons Attribution-NonCommercial-NoDerivatives 4.0 International (CC BY-NC-ND 4.0) License.